

Algorithm Theoretical Basis Document

Hydro-Estimator (Modified)

Atul Kumar Varma and R M Gairola

Geophysical Parameter Retrievals Division
Atmospheric and Oceanic Sciences Group
Space Applications Centre, ISRO
Ahmedabad 380015, India

March 2015

Document Control and Data Sheet

1	Date	March 04, 2015
2.	Title:	Algorithm Theoretical Basis Document: Hydro-Estimator (Modified)
3.	Version	1.0
4.	Document No.	SAC/EPESA/AOSG/SR/04/2015
5.	Type of Report:	scientific Note
6.	No. of Pages:	29 (including title page)
7.	Author:	Atul K Varma and R M Gairola
8.	Originating unit:	GRD/AOSG/EPESA/SAC, Ahmedabad 380058.
9.	Abstract:	<p>The Hydro-Estimator (H-E) is a INSAT-3D based high resolution rain estimation method which combines NCEP model parameters with satellite observations. The Hydro-Estimator developed at SAC is based on similar operational method at NOAA/STAR. The H-E is operationally implemented. This report addresses the validation of H-E in the present form. It is found that the H-E in its present form works well over most parts of the country but has weakness over hilly terrains. The problem is identified and a modified H-E is proposed. The modified H-E shows a good representation of rain over hill terrains. Overall, it gives a correlation of 0.78 and rms difference of 46.64 mm when compared with weakly meteorological subdivision surface measurements. Its comparison with TRMM 3B42 V7 also provides the same correlation and rms difference. It is also found that comparison statistics of weekly met subdivision averaged surface observations with H-E is nearly same as that with 3B42 V7. However, the week-by-week comparison of surface measurements with H-E is more stable than with 3B42 V7. In daily 0.25°x0.25° grid, the correlation and rms difference over land between surface observations and H-E is 0.47 and 25.40 mm/day. A slightly higher correlation of 0.59 and lowered rms difference of 22.40 is observed between H-E and 3B42 V7. These comparison statistics are in agreement with comparison of surface observations with 3B42 V7. The similar comparisons over oceans are conducted between H-E and 3B42 V7, which show a correlation of 0.65 and rms difference of 15.88 mm/h. The advantage of H-E over 3B42 V7 is its near real time dissemination. Report provides details of the study.</p>
10.	Classification:	Unrestricted
11.	Distribution:	All concerned

Algorithm Theoretical Basis Document: Hydro-Estimator (Modified)

Atul Kumar Varma and R M Gairola
Geophysical Parameter Retrievals Division
Atmospheric and Oceanic Sciences Group
Space Applications Centre, ISRO
Ahmedabad 380015, India

1.0 Introduction

Conventionally rainfall over the ground is measured using rain gauges and radar. Rain gauges offer point measurements and thus they do not represent spatial variability of the precipitation that varies from few meters to several kilometers. The distribution of the rain gauges is far from adequate to present the meaningful variability for the study of various rain-induced events/processes, like flash flood, dam failure, river catchment, etc. On the other hand, radars are better representative of the areal rain, but their coverage is limited due to their high cost. The radar measurements often suffer due to poor calibration of radar reflectivity and also of Z_e -R relationship. Apart from that, ground clutter and anomalous propagation also mars its usability. At the time of severe weather conditions, ground based observation network often fail to work. In view of the limitations of the ground measurements, the most convenient means to measure the precipitation over large area is by using the satellite-based methods. The satellites offer frequent uniform coverage over large area. However, the satellite measurements also suffer from large errors. While Vis./IR methods suffer from their inability to sense hydrometeors directly (Bhandari and Varma, 1995), microwave measurements suffer due to their coarser spatial and temporal resolution, rain variability within their large footprint referred as beam filling problem, uncertainty in the drop-size distribution, drop temperature, fall velocity and shape and orientation of the drops etc. (Varma et al, 2003, Varma and Liu, 2006, Varma and Liu, 2010, and Varma and Pal, 2012).

Due to inherent inability of IR measurements to directly sense the hydrometeors, the rain retrieval using them is always indirect in nature. In the past, there are a number of methods developed for rain estimation (barrett and Martin, 1981); they range from very simple algorithms in which brightness temperature (T_b) is directly related to rain rate (e.g., Arkin et al., 1989) to those which involved complex hypothetical models (e.g., Scofield, 1987). Scofield (1987) described a method for measuring the intense precipitation over a storm. His method called Interactive Flash Flood Analyzer (IFFA) that used half-hourly satellite images to measure the precipitation over the active area of a storm. His technique involved the skill of a trained meteorologist to find out active portion of a storm. He also utilized the total atmospheric precipitable water (TPW) and water vapour (WV) correction to make modifications for dry/wet environment and equilibrium level adjustments for rain that comes from the warm clouds. This method was found to be successful for measuring precipitation but was highly subjective and needed continuous interaction of a trained meteorologist to decide the precipitation amount. Thus, it was found difficult to implement it with ease. Successively, an alternate method called Auto-Estimator (A-E) was developed. The aim of the A-E was to

provide an automated method without human intervention and that could automate the subjective nature of the IFFA, but A-E failed on many occasions because many features of IFFA were not properly implemented in it. Hydro-Estimator is most recent of the attempts by NOAA/NESDIS to improve and make IFFA automated (Scofield and Kuligowski, 2003). The H-E incorporated many new features that were either not present in IFFA or were defined differently.

A brief summary of the Hydro-Estimator is provided in section 2 below. Further details of Hydro-Estimator technique can be found in Algorithm Theoretical Basis Document (ATBD) (Varma and Gairola, 2013).

2.0 Hydro-Estimator

The H-E method offers improvement over A-E method for precipitation estimation. In A-E method, the relationship between 10.7 μm brightness temperature (T_b) and rain rate (mm h^{-1}) (R) is defined as:

$$R = a \exp(-bT_b^{1.2}), \quad \text{-----(1)}$$

where, a and b are regression coefficients having values $a = 1.1183 \times 10^{11}$; $b = 0.036382$ (Vicente et al. 1998). The A-E method provides same relationship for core and non-core precipitation. The above equation provides first guess of the precipitation value for core rain and is hereafter referred as (R_c). In H-E, the rain is determined by the cloud growth at the given pixel relative to the surrounding pixels. The H-E method ensures heavier rain for growing clouds, in the upwind portion of the storm with overshooting tops. The core and non-core fractions of the precipitation are identified and different R - T_b relationships are provided for them. This allows higher precipitation rates for the convective cores. For convective core, an equation similar to (1) is used, however the coefficients a and b are dynamic in nature, and which depends upon available TPW as provided by National Centre for Environmental Predictions (NCEP/NOAA) Numerical Weather Prediction (NWP) model derived fields. This allows higher precipitation value for wetter atmosphere. The above (1) is constrained with precipitation value of 0.5 mm h^{-1} at $T_b = 240 \text{ K}$, and a precipitable water (from NCEP model) dependent value at $T_b = 210 \text{ K}$. In H-E method, the maximum possible rain at any pixel is limited depending upon availability of TPW. This allows the maximum precipitation as a function of available moisture. The maximum possible rain value in mm/h is restricted to 40 times the precipitable water in inches.

If a pixel is assigned maximum rain but there exist a colder pixel in its vicinity. In principle, the rain rate at the colder nearby pixel would be higher. Thus the rain rate curves are recomputed based on rain rate of 0.5 mm/h at 240 K and of the theoretical maximum value at the lowest temperature in the vicinity.

For a non-convective core, the relationship between T_b and R_n is given as:

$$R_n = (250 - T_b) * (R_{\text{max}}/5) \quad \text{-----(2)}$$

R_{max} is again a function of PW. R_n is not allowed to exceed - corresponding R_c rain rate or 12 mm/h, whichever is lower.

In H-E method, the precipitation at a pixel is considered to comprising of core and non-core fractions. This is worked out by considering an area of 101X101 pixels surrounding the pixel under consideration. The minimum, mean and standard deviation of Tb (T_{min}), in this area is determined. This T_{min} is used to find the radius of actual region of interest. Within this radius of interest, the mean (T_{mean}) and standard deviation (σ) of Tb are determined. The active/inactive and also core/non-core fraction of the pixel is determined through the parameter Z,

$$Z = (T_{mean} - T_b) / \sigma \quad \text{-----}(3)$$

The minimum and maximum allowable value of Z are 0 and 1.5.

If $Z < 0$; H-E rain (R) = 0, i.e., pixel either cirrus or inactive convective

$$\text{Otherwise, } R = [R_c * Z^2 + R_n * (1.5 - Z)^2] / [Z^2 + (1.5 - Z)^2] \quad \text{-----}(3)$$

R_c is the rain from the convective core given by (1) with coefficients determined by PW from NCEP NWP model. R_n is rain from non-convective core given by (2). If $Z=1.5$, the pixel rain rate R reduces to convective type only (given by (1)). On the other hand, if $Z=0$, the pixel rain rate R is determined by purely non-convective rain (given by (2)).

In fact, the convective systems generally have multiple brightness temperature minima, and hence a single radius is inappropriate for differentiating local from global minima. Thus, this same computation of rain rate is performed for a smaller (15-pixel) radius, and the final rain rate is the square root of the product of the two rates. The exception to this is if the rain rate computed from the smaller radius is zero, in which case it is not considered in the final rain rate calculation.

The (3) above provides the first guess precipitation amounts. The precipitation thus estimated is further modified to account for the wetness/dryness of the atmosphere and also for the precipitation that comes from the warm clouds. The several steps involved for such modifications are as follows:

2.1 Correction for Wet/dry Environment

A small correction in the brightness temperature (Tb) values is carried out to account for wetness of the environment. This adjustment is needed to account for evaporation of the precipitation in the dryer environment below the cloud. A higher or lower value of the brightness temperature at 10.7 μ m is set for drier or wetter environment. This is carried out in two steps. In the first step, brightness temperature is adjusted based on the TPW value to compute rain rate from (3). In the second step, first, the relative humidity (RH)

itself from the NCEP model is adjusted to account for the falling rain, and then depending upon RH value, a subtraction from the rain amount given by (3) is made.

2.2 Warm-top modification

The equilibrium level or Level of Neutral Buoyancy (LNB) is computed by following a parcel along a saturation adiabat upward (from lifting condensation level) to where the parcel temperature becomes equal to the environmental temperature. Strength of the convection is determined by a comparing the temperatures of the convective tops with that of equilibrium level. This level lies below tropopause for the warm rain.

In H-E method, NCEP model temperature and dewpoint profiles are used to determine equilibrium temperature (T_{eq}) of a particulate pixel. This correction is applied to pixels that are warmer than the equilibrium level temperature.

- If the $(T_{eq} - T_{min}) < 10$ K, then T_{min} in the pixel-area is used instead of T_b of the pixel for warm top correction. The modification is as follows:

$$T_b - [(213 - T_{eq}) * 0.9] \text{ or } 25 \text{ K (whichever less)}$$
- If the $(T_{eq} - T_{min}) > 10$ K, the modification is as follows

$$T_b - [(213 - T_{eq}) * 0.6] \text{ or } 15 \text{ K (whichever less)}$$

2.3 Orographic Correction

Corrections for the orography induced rain and the rain from warm clouds are also applied. This correction is carried out to ensure enhanced rain amounts along windward side and reduced rain amounts along leeward side of the mountains. The orographic correction is carried out by determining by gradient of the elevations in the direction of the prevailing 850 mb level winds (Vicente et al., 2002).

3.0 Sample Results and comparisons

The H-E method which is currently operational at Indian Meteorological Department (IMD) and Indian Space Research Organisation (ISRO) uses INSAT-3D Imager thermal infrared (TIR) observations at $10.7 \mu\text{m}$ along with environmental parameters taken from Numerical Weather Prediction (NWP) model to make a quantitative assessment of the precipitation. The H-E technique provides rain rate at each pixel with every acquisition of the satellite data (presently, $4 \times 4 \text{ km}^2$ and 30 minutes for INSAT-3D). The procedure and coefficients are adopted from H-E method developed by NOAA/STAR.

Hydro-Estimator performed reasonably well over the land and oceans. As an example, Fig. 1 shows the instantaneous H-E rain on 23 September 2013 at 1200 UTC from INSAT-3D along with H-E rain as derived by NOAA using Meteosat and rain from TRMM 3B41RT. There is a good qualitative agreement between rain rates derived using INSAT-3D and Meteosat. Though H-E rain by NOAA and by us uses the same

technique and coefficients, the difference between the two methods still exists due to their different inputs. While INSAT-3D based H-E algorithm used $0.5^{\circ} \times 0.5^{\circ}$ gridded 6 hourly NCEP Global Forecasting System (GFS) model derived parameters whereas NOAA algorithm uses high-resolution ETA model derived fields. Nevertheless, there is good qualitative agreement between H-E rain derived from INSAT-3D and Meteosat. There is also fairly good qualitative agreement between H-E rain from INSAT-3D and from 3B41RT. The 3B41RT is microwave based hourly rain rates.

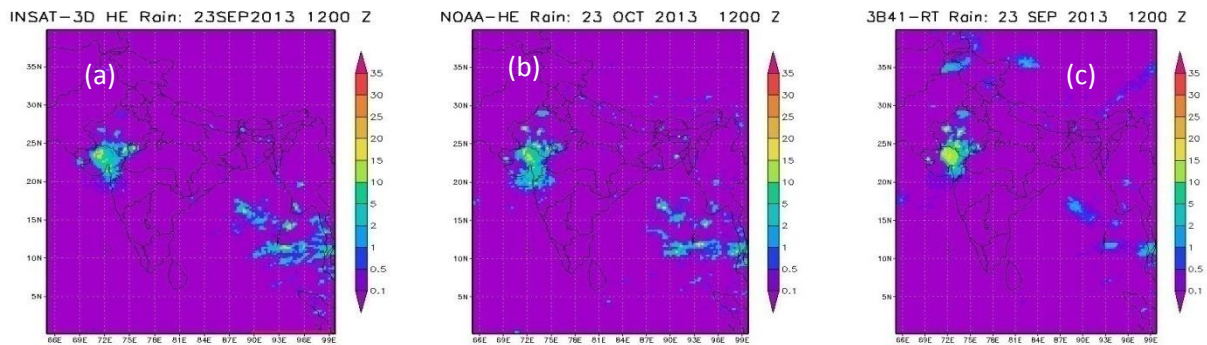


Fig.1: Rain rate in (mm/h) on 23 Sep. 2013 at 1200 UTC from (a) INSAT-3D by SAC, (b) GMS by NOAA and (c) TRMM 3B41RT.

Despite of having good agreement over most of the regions, the rain over the Himalayan region is not well picked up by H-E rain from INSAT-3D as well as from Meteosat. This issue is dealt in modified H-E that is described in the later part of this report.

Figure 2 show another example of INSAT-3D derived instantaneous H-E rain associated with Phailin cyclone from 10 – 13 Oct. 2013. The Fig. 2 (a) to (h) shows the development to decay of the cyclone in chronological order. The intense rain associated with eye-wall as well as spiral clouds bands of the cyclone is clearly seen. The H-E also very well picked up the eye of the cyclone as rain-free area. The distribution as well as the intensity of the H-E rain associated with cyclone is found to be in agreement with the observed history of the cyclone (Anonymous, 2014).

The cyclone made a landfall on 12 Oct. 2013 at around 1530 UTC and caused intense rain in Orissa during 12-14 Oct 2013. The Figure 3 show the district averaged rain rate from H-E and a network of rain gauges from the state government of Orissa. A good agreement can be observed in rain distribution from H-E and surface observations.

A scatter plot of H-E rain and surface observations from Fig. 3 is shown in Fig. 4.

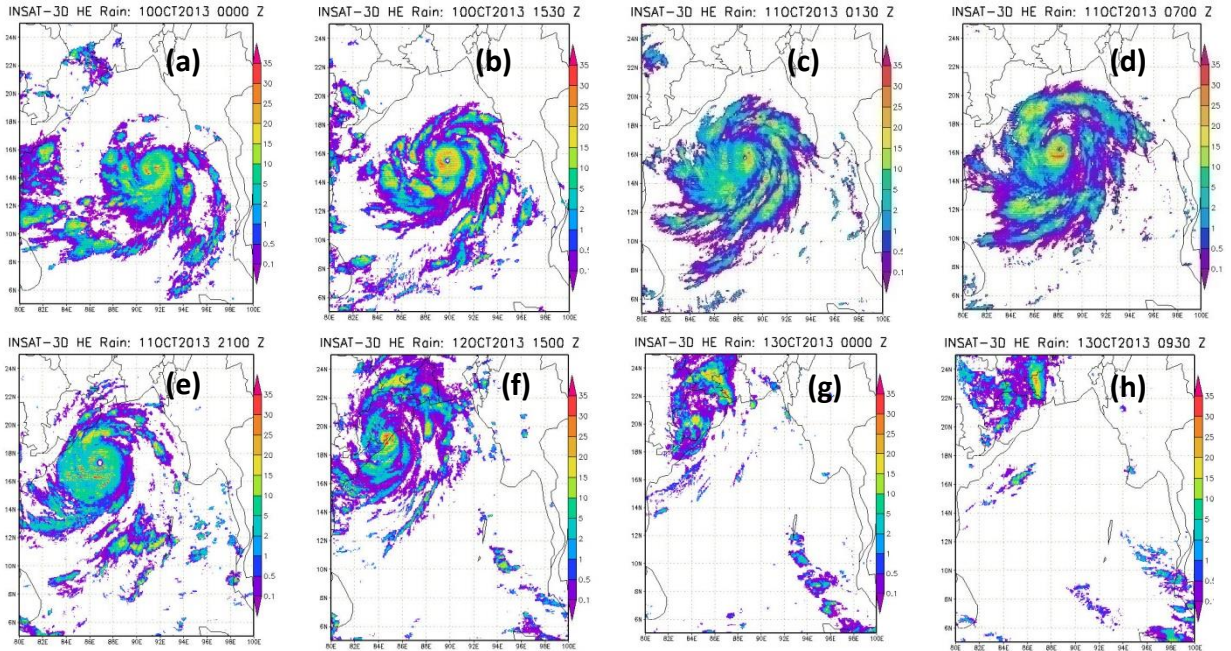
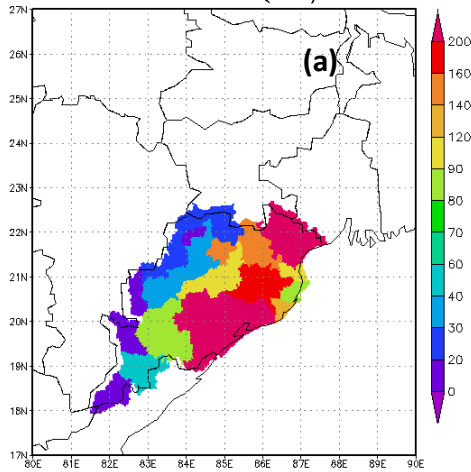


Fig. 2: Chronological history of rain rates associated with Phailin cyclone from INSAT-3D based Hydro-Estimator method.

12-14 Oct 2013 District Rain (mm)from INSAT-3D HE



12-14 Oct 2013 District Rain (mm)from surface Obs.

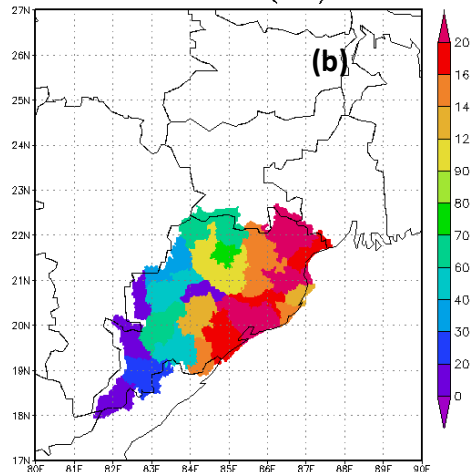


Fig. 3: Distribution of the district average rain for the Orissa from (a) H-E and (b) surface observations.

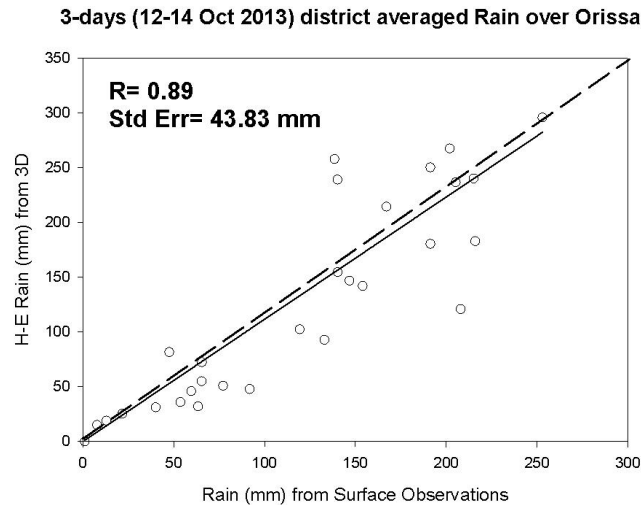


Fig. 4: Scatter plot of 12-14 Oct 2013 district averaged rain from Orissa from H-E and surface observations.

The 3-days, 12-14 Oct. 2013, Orissa state averaged rain associated with the Phailin cyclone from INSAT-3D H-E, surface observations, TRMM-3B42RT and CPC is provided in Table 1.

Table 1: Orissa state averaged rain associated with Phailin cyclone from 12-14 Oct. 2013.

Rain (mm)			
H-E	Surface Obs.	3B41RT	CPC
125.89	110.1	60.0	180.0

Thus it can be concluded that INSAT-3D H-E rain is not only in a good qualitative and quantitative agreement with surface observations but it is also having a good agreement in its spatial distribution.

Further, we have compared weekly meteorological (met) subdivision averaged rain from INSAT-3D H-E with corresponding rain values from IMD generated weekly weather reports (WWR) and TRMM-3B42RT for 7 weeks from 29 May to 16 July 2014 of the S-W monsoon season. The Fig. 5 shows the inter-comparison of weekly met-subdivision averaged rain from H-E, WWR and 3B42RT.

The Fig. 5 shows a reasonably good agreement of H-E weekly rain with IMD WWR and TRMM-3B42RT. To examine the comparison statistics of H-E rain in better perspective, we have provided the comparison of 3B42RT with IMD WWR. It may be recalled that 3B42RT is an IR and microwave merged product.

Further comparison is made between hourly CPC 1°X1° latitude-longitude gridded rain with H-E rain for period from 23-27 October 2013. The comparison statistics is provided in Table 2 below. For comparison in smaller spatial and temporal scales, a comparison

of INSAT-3D H-E with TRMM 3B41RT hourly rain in $0.25^{\circ} \times 0.25^{\circ}$ latitude-longitude grid is made for period 20-24 Sep 2014. The TRMM 3B41RT is a microwave derived rain product and is available hourly.

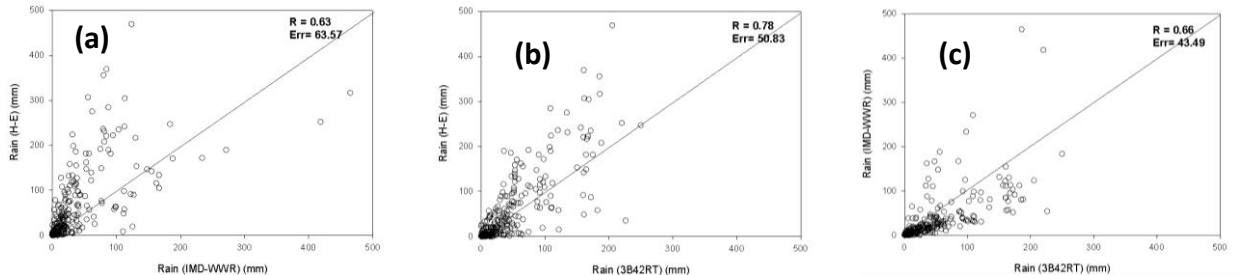


Fig. 5: Comparison of weekly meteorological sub-division averaged rain for 7 weeks from 29 May to 16 July 2014 between (a) IMD WWR and H-E rain, (b) TRMM-3B42RT and H-E rain, and (c) TRMM 3B42RT and IMD WWR.

Table 2: Comparison statistics of rain from H-E with CPC and 3B41RT

Comparison between CPC and INSAT-3D H-E Rain					
Period	Time Scale	Spatial Grid	R	Rmsd	Bias
23-27 Oct 2013	Daily	$1^{\circ} \times 1^{\circ}$	0.69	17.01 mm	3.13 mm
Comparison between 3B41RT and INSAT-3D H-E Rain					
20-24 Sep 2014	Hourly	$0.25^{\circ} \times 0.25^{\circ}$	0.59	1.06 mm/h	0.12

4.0 Need for further Improvements in Hydro-Estimator

The results presented in section 3.0 above show a reasonable good agreement between H-E rain and surface observations. The most of the result presented in the above section are dominated by regions that are either oceans or have moderate elevations from the sea level. Figure 6 below shows the comparison of IMD Weekly WWR met-subdivision accumulated rain for 7 weeks with corresponding H-E rain averaged over 4 typical high orographic met-subdivisions, viz. Arunachal Pradesh (AP), Uttarakhand (UK), Himachal Pradesh (HP) and Jammu and Kashmir (J & K),

The Fig. 6 shows that H-E rain estimated for areas with high altitudes is largely underestimated with respect to surface observations. Also, with regard to Fig. 1, as it is already mentioned in section 3.0 that the rain over Himalayan region is not well depicted by H-E rain from INSAT-3D as well as that provided by NOAA using Meteosat. In view of the observed underestimation of the rain by H-E in the present form over high altitude regions, it is desired to investigate its possible reason and accordingly modify the H-E method to make it able to better represent the rain over high altitudes.

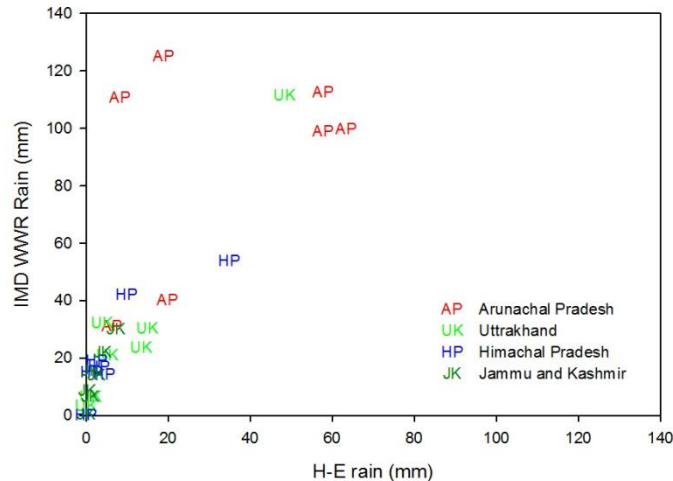


Fig. 6: Comparison of IMD weekly rain from WWR with corresponding H-E rain in 4 met subdivisions with high altitudes.

5.0 Modified Hydro-estimator:

As discussed the previous section, the H-E is not able to give satisfactory measurements over high altitudinal regions. This weakness of H-E is noticeable despite of the fact that the H-E method is designed with corrections for orography and warm rain. Herein we reinvestigated different corrections applied to the H-E method to work out procedures to make it better representative of surface observations, especially in high altitudes.

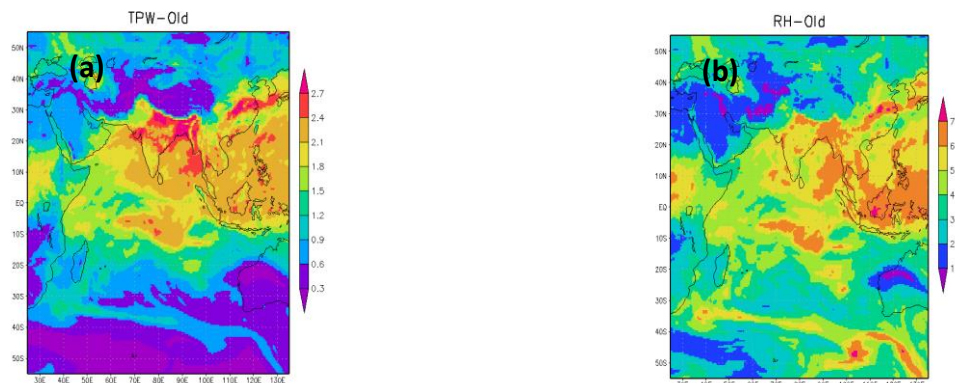


Fig. 7: NCEP GFS model derived (a) TPW and (b) RH for a typical day and time.

Correction of NCEP derived TPW and RH

It was observed in the NCEP GFS analyzed fields that TPW and RH values are very low in the Himalayan region. For example, Fig. 7 shows the TPW (in inch) and RH (in percentage) for a typical day and time, which shows very low value over Himalayan region. Such low values of TPW and RH in NCEP GFS fields are observed irrespective of date and time of the observation. Such low values are not supportive of the high rain rates in H-E method and hence the estimated rain is largely underestimated.

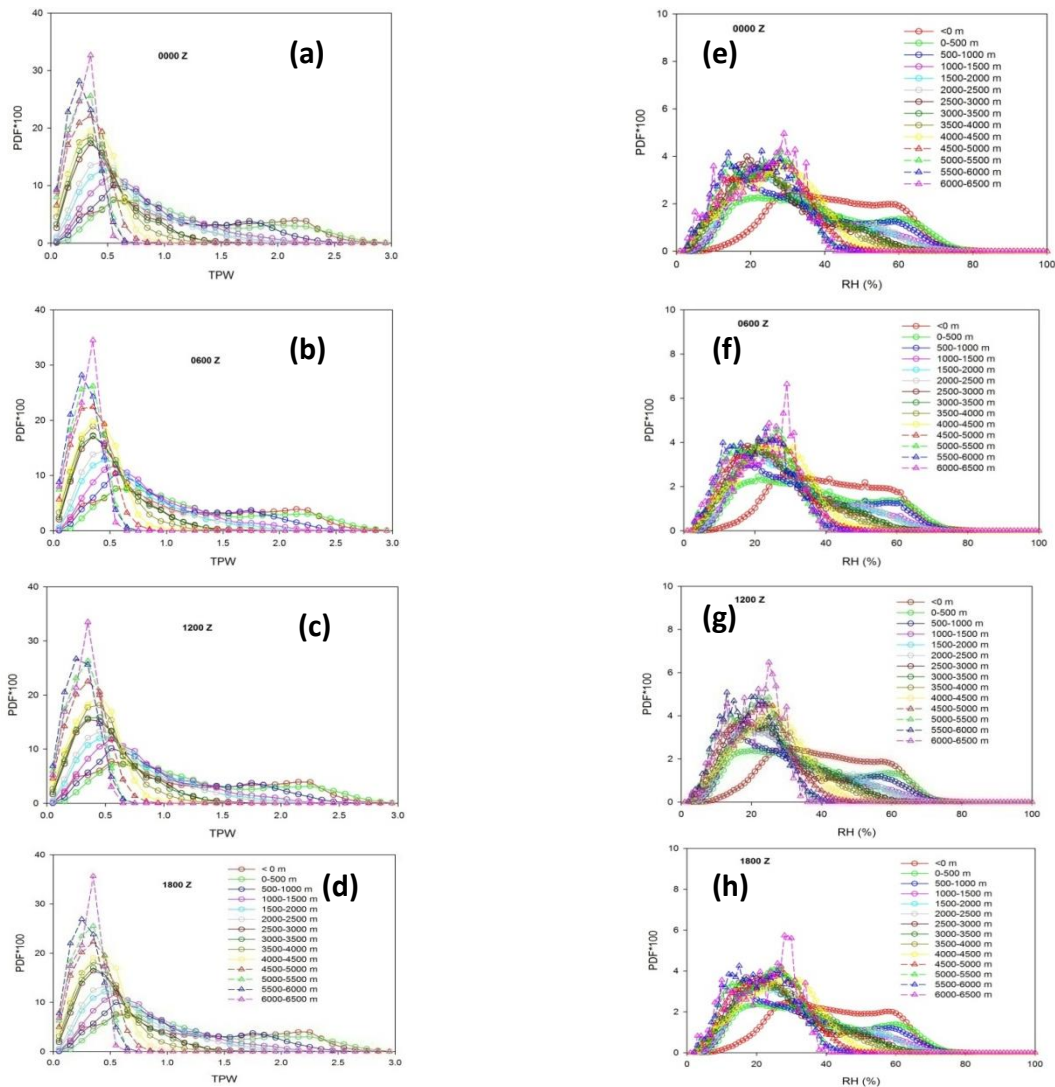


Fig. 8: Conditional probability distributions using July 2014 NCEP GFS model derived fields over Indian region of TPW (inch) at (a) 0000 UTC, (b) 0600 UTC, (c) 1200 UTC and (d) 1800 UTC, and RH (percentage) at (e) 0000 UTC, (f) 0600 UTC, (g) 1200 UTC and (h) 1800 UTC.

In order to examine, TPW and RH values with respect to altitude, we have plotted conditional probability distributions (PDF) of TPW (in inch) and RH (in percentage) conditioned to different altitudes over Indian region (i.e., 0-40 N and 65-100 E) from one full month (July 2014) of NCEP GFS analyzed fields separately for each of the observation times (i.e., 0000, 0600, 1200 and 1800 UTC). This is shown in Fig. 8. In which it can be seen that TPW and RH have nearly same PDFs irrespective of time of observation. Also the TPW and RH values are always very low at high altitudes. For example, for altitude above 4000 m, the TPW is always less than 1 inch and RH is always less than 50%. In order to have their values at higher altitudes comparable to that at lower altitudes, we have carried out histogram matching with respect to their

corresponding values between 0-500 m values. By histogram matching we intend to make their probability of occurrence same at all altitudes. The Fig. 9 shows the corresponding PDF values before and after histogram matching.

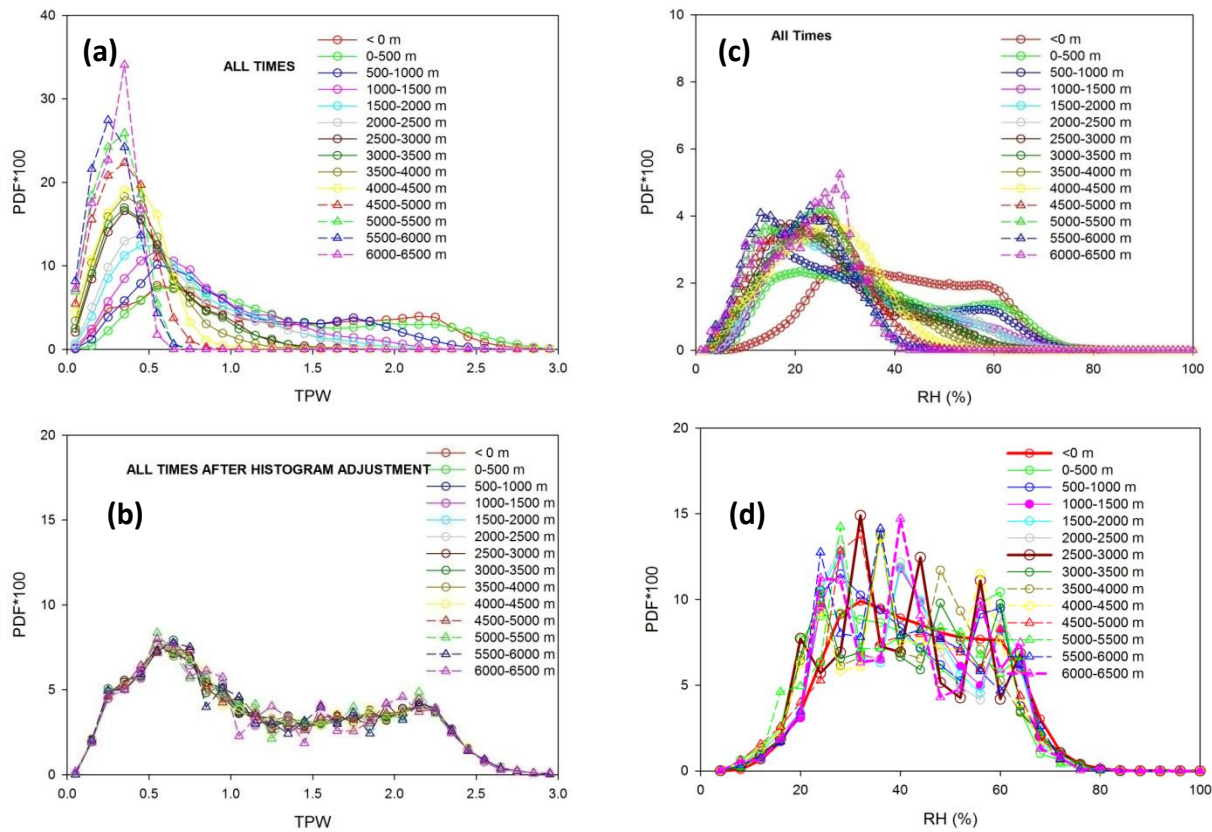


Fig. 9: Probability distributions at different altitudes with one month of NCEP GFS model fields at 0000, 0600, 1200 and 1800 UTC of (a) TPW, (b) TPW after histogram equalization, (c) RH, (d) RH after histogram equalization.

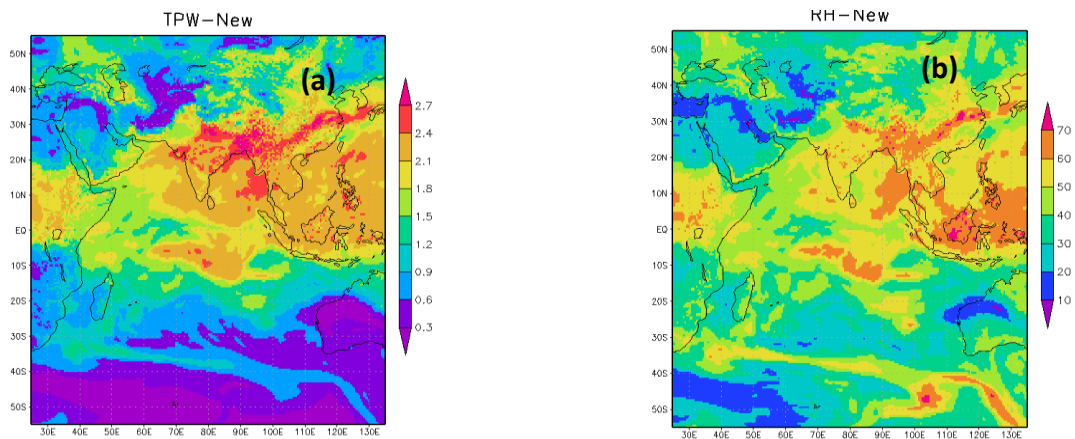


Fig. 10: (a) TPW, and (b) RH after applying histogram equalization to values in Fig. 7.

Figure 9 (a) and (c) show the conditional PDFs of TPW and RH with all time data from Fig. 8 and Fig. 9 (b) and (d) show them after carrying out histogram equalization. The Fig. 9 shows that with histogram equalization the probability of occurrence of TPW and RH value is nearly same irrespective of altitude. The correction based on histogram equalization (Fig. 9) is applied to TPW and RH values shown in Fig. 7. The modified TPW and RH values are provided in Fig. 10. The Fig. 10 looks similar to Fig. 7 except corresponding values over Himalayan region which are now have higher values compared to those in Fig. 7. We expect that this correction in TPW and RH will help getting more representative rain values from H-E.

5.1 Correction of Equilibrium Level / Level of Neutral Buoyancy Computation

The Equilibrium Level (EL) or Level of Neutral Buoyancy (LNB) is computed by following a parcel along a saturation adiabat upward (from lifting condensation level) to where the parcel temperature becomes equal to the environmental temperature. Strength of the convection is determined by a comparing the temperatures of the convective tops from IR measurements with that of EL. This level comes before tropopause for the warm rain. This adjustment was initially developed to enhance rainfall in regions where the convective EL was too low (in height) for very cold cloud tops to develop, but where very heavy precipitation is still possible.

If equivalent potential temperature of the parcel is θ_e and saturated equivalent potential temperature of the environment is θ_{es} , then usually a parcel begins with $\theta_e < \theta_{es}$ of the environment. As the parcel rises, conserving θ_e , it will eventually have a θ_e equal to the θ_{es} of the environment; this is referred as the level of free convection (LFC). As the parcel rises above the LFC, it is positively buoyant and will continue to raise until eventually θ_e is equal to the θ_{es} of the environment again, this is referred as EL or LNB. Above the LNB the parcel becomes negatively buoyant and tends to return to the LNB. Assuming adiabatic ascent, i.e., no mixing of environmental air, we can determine the LNB for given sounding.

Conventionally, the θ_e and θ_{es} are determined considering 1000 mb as the reference level. We find that by taking 1000 mb as reference the convergence of thermodynamic equations above hilly terrain is not always possible, and thereby it does not allow us to carry out correction for warm rain over such regions. Taking cognition of the fact that 1000 mb is not a realistic level over hilly terrain where surface pressure is often much lower. We thus replaced this 1000 mb with surface temperature over hilly terrain in thermodynamic equations for θ_e and θ_{es} . This resulted in more often convergence of equations over hilly terrains. Figure 11 (a) shows the EL/LNB as computed using 1000 mb as reference surface and Fig. 11 (b) shows the EL/LNB as computed with modified algorithm. One can notice the changes only over some regions (especially, Himalayas, Hindukush and Arabia) where with modified scheme the computation of LNB is now possible.

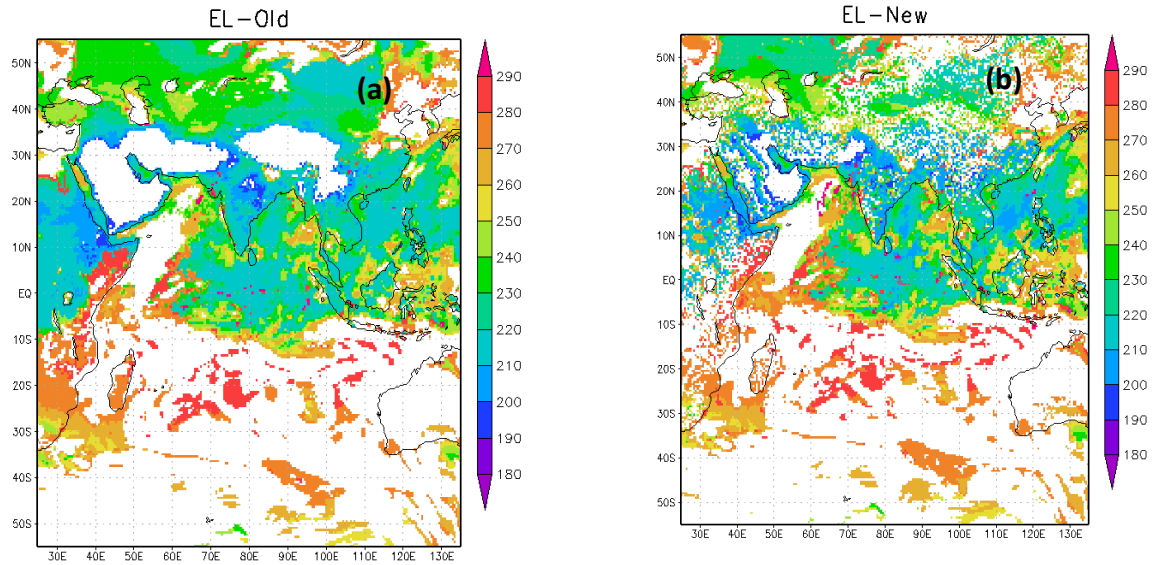


Fig. 11: LNB calculated with Temperature and RH vertical profiles from NCEP GFS model fields with (a) 1000 mb as reference surface, (b) actual surface pressure.

5.2 Modification in orographic correction

The orographic correction uses 850 mb wind speed which is unrealistic level over high altitudes. The 850 mb level is considered for avoiding the boundary layer for surface pressure close to 1000 mb level. For high orographic regions, this needs to be modified and replaced with realistic level. This is done in the modified algorithm; we can see the 850 mb u-wind component on a typical date and time in Fig. 12 (a), and modified wind input to orographic correction in Fig. 12 (b). One can see the moderate changes in the wind only over orographic regions.

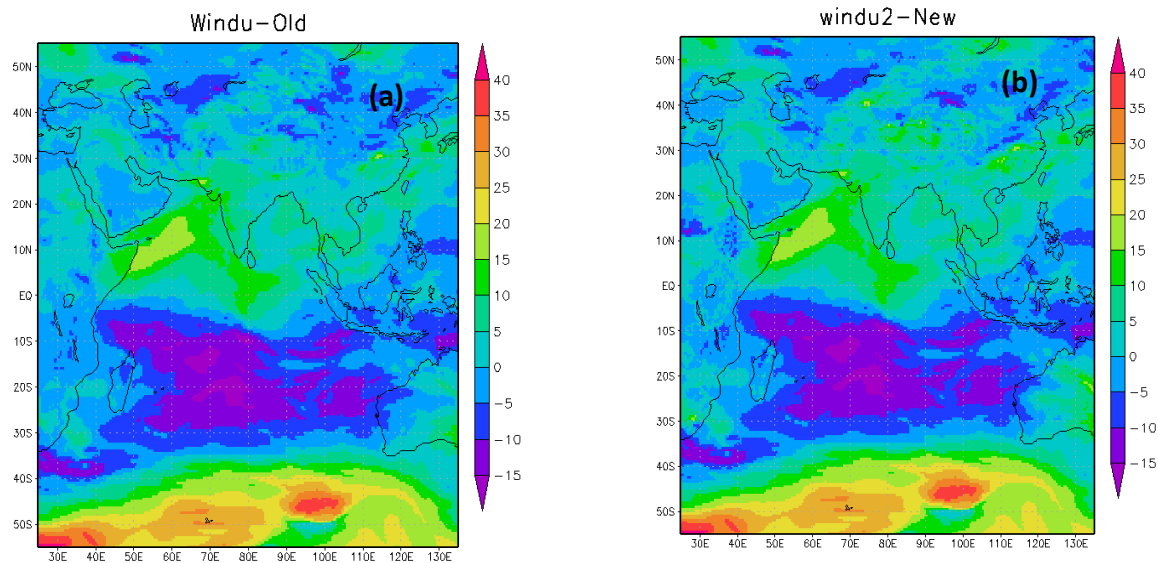


Fig. 12: From NCEP model fields (a) Wind Speed at 850 mb (b) Wind Speed above boundary layer.

With above modifications, we examined the capability of H-E for measuring intense rain over Himalayas. Few examples are presented in the next section. We have presented a detailed validation of the modified H-E over all the other regions too.

6.0 Validation of Modified Hydro-Estimator

The above modifications in H-E are aimed at improving rain over orographic regions. Hence the success of the changes in the H-E depends primarily on its improved performance over Hilly terrain, and its consistent or improved performance over all other regions. We have taken two different cases of intense rain over Himalyas which were poorly represented by H-E. One is that of flash floods in Utrkhand from 15-17 June 2013 which resulted heavy flooding and huge loss of life and property. In June 2013, INSAT-3D was not available and hence we applied the modified algorithm to Kalpana-1 VHRR observations and examined the performance. Figure 13 shows the rain over Utrkhand region in the morning of 17 June 2013 when scores or people were perished in Kedarnath, Badrinath and other adjoining regions. The Fig. 13 (a) is H-E rain measurements without applying modifications and Fig. 13 (b) shows the H-E rain with modifications as described in section 5.0. We can see the mark difference in the rain intensity with corrections.

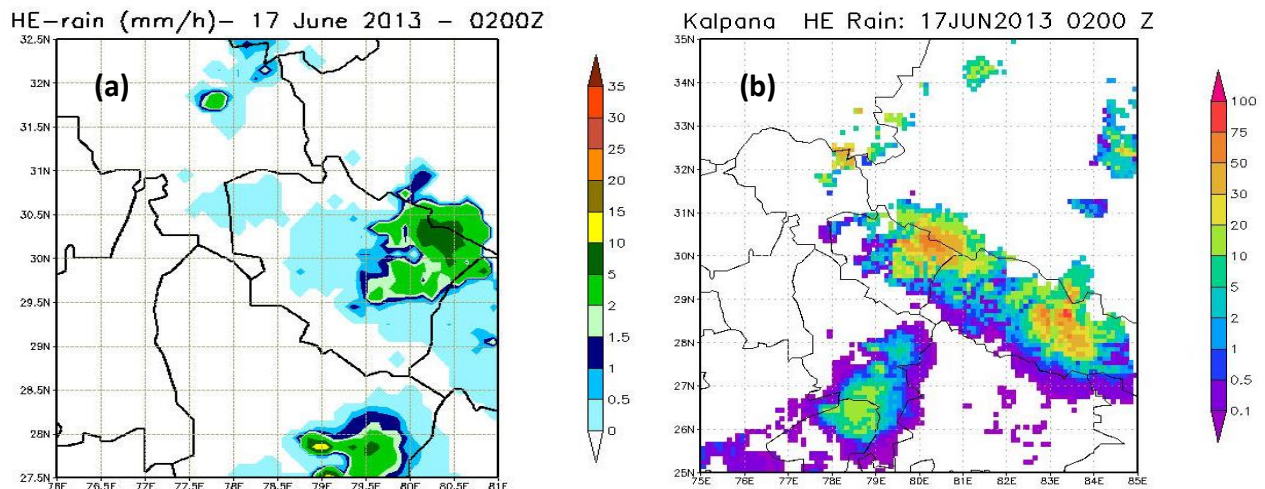


Fig. 13: H-E rain in Utrkhand on 17 June 2013 at 0200 UTC (0730 IST) (a) without modifications, (b) with modifications.

The Fig. 14 (a) show the weekly averaged 13-19 June 2013 district rain from modified H-E. The state averaged rain from H-E is 316 mm. The Fig. 14 (b) is weekly averaged rain map for the same week from IMD WWR, which shows a value of 322.9 mm for the state of Utrkhand. Thus, H-E with modifications provided in section 5.0 is able to give a very close to realistic weekly rain values over Utrkhand.

State Average from modified H-E: 316 mm

State Average from IMD WWR: 322 mm

(a)



(b)

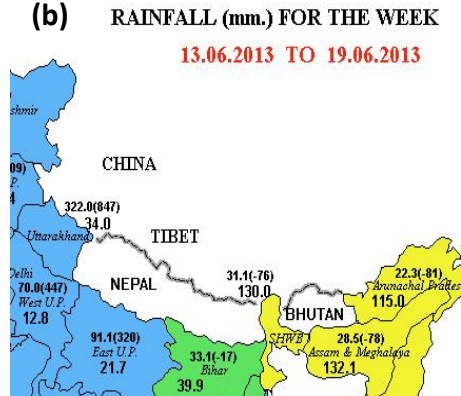


Fig. 14: Averaged rain for a week from 13-19 June 2013 (a) district averaged from modified H-E, (b) IMD Weekly Weather Report.

The other case of intense rain over Himalayan regions that is presented here is that of intense rain and floods in Jammu and Kashmir during 3-5 September 2014. Figure 15 (a) shows the rain from INSAT-3D H-E on 04 September 2014 at 1500 hr without applying modifications. It can be observed that modified H-E is able to capture very intense rain in the Jammu and Kashmir (J&K) region (Fig. 15 (b)), which otherwise it is not able to capture in Fig. 15(a).

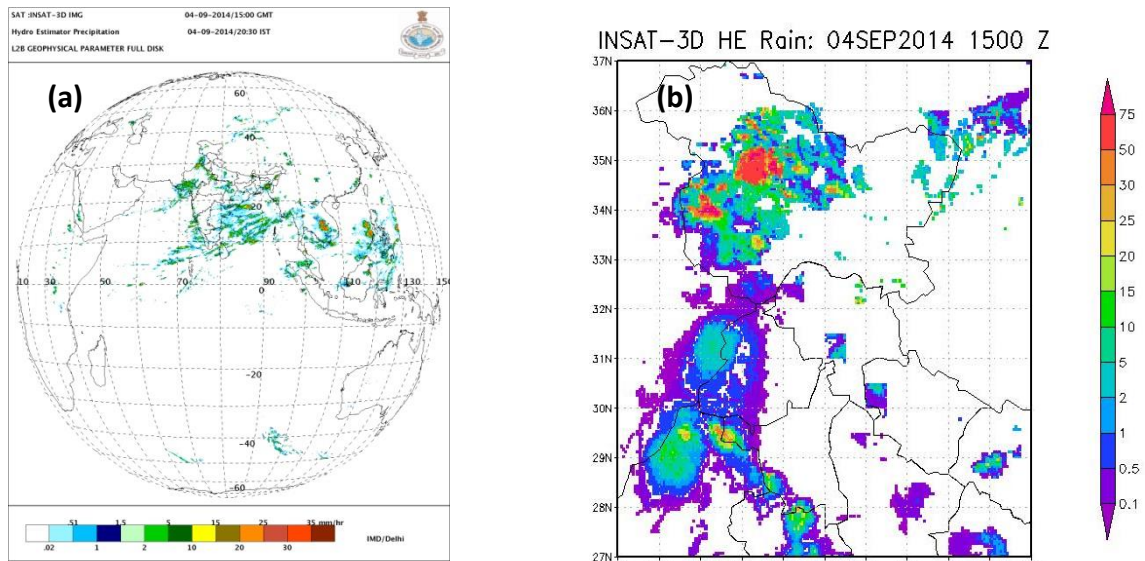


Fig. 15: Rain on 04 September 2014 at 1500 UTC from (a) without modification, and (b) with modification.

The J&K state averaged H-E rain from modified algorithm for week from 3-10 September 2014 is found to be of 245.78 mm which is very close to the IMD WWR provided rain of 267.7 mm. For the same week TRMM-3B42 V7 provides corresponding rain value of 95.33 mm. Thus the H-E rain from modified algorithm is better representative of intense rain in J&K during 3-10 September 2014 than TRMM 3B42 V7.

The above two case studies of very intense rain over hilly terrain gives us confidence that the modifications in H-E method as described in section 5.0, give more representative rain values over Hilly terrain.

Further validations are carried out of the modified algorithm in different spatial and temporal scales with IMD daily gridded, weekly met-subdivision averaged (from WWR) rain values, and also with TRMM 3B42 V7, which is an IR and microwave merged product.

We have computed the H-E rain from modified algorithm for 10 week period from 3 July to 10 September 2014. The rain values are averaged in met-subdivisions on weekly basis and compared with rain values provided by IMD in WWR. A scatter plot of comparison is shown in Fig. 16.

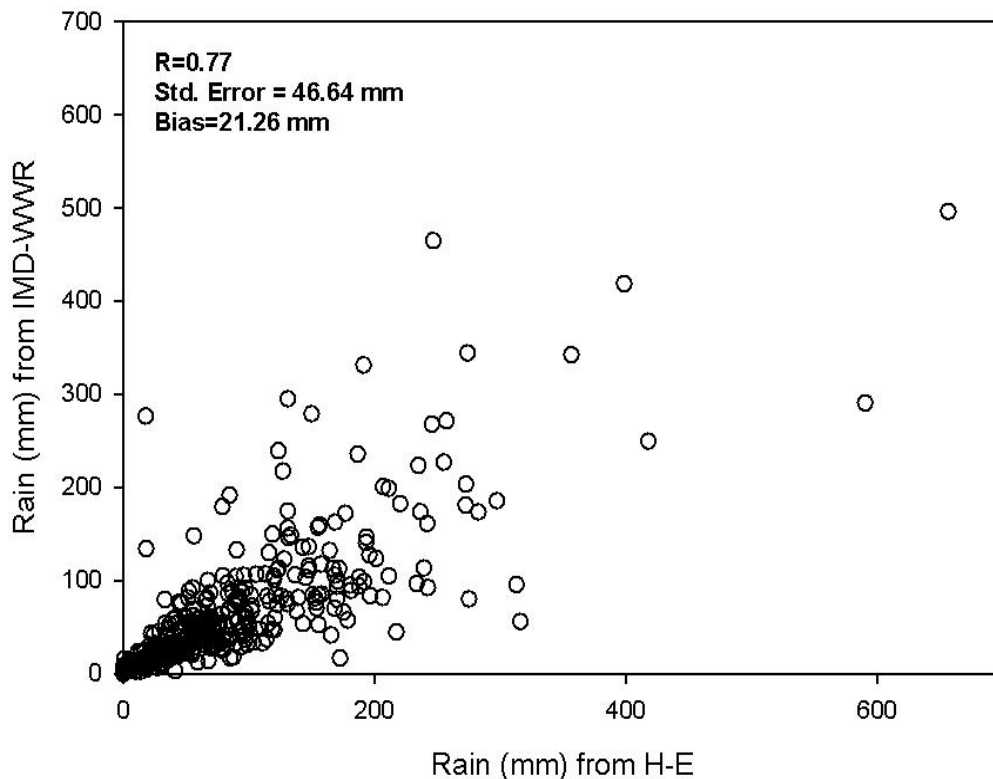


Fig. 16: Comparison of weekly meteorological subdivision averaged rain from H-E and IMD WWR for 10 weeks from 3 July to 10 September 2014.

The Fig. 16 when compared with Fig. 5 (a), shows a marked improvement in the comparison of H-E rain with WWR rain values, both in terms of correlation as well as standard deviation of their difference. This is despite of the fact that range of the rain values plotted in Fig. 16 is higher compared to that in Fig. 5 (a).

The Fig. 16 provides statistics of comparison for all the 10 weeks of comparison, the week-by-week comparison statistics is provided in Table 3 below.

Table 3: Week-by-Week comparison statistics of weekly meteorological subdivision averaged H-E rain with IMD WWR.

Week ending on	HE Vs IMD WWR		
	R	Err	Bias
9 July 2014	0.80	40.93	20.29
16 July 2014	0.74	86.62	47.98
23 July 2014	0.64	92.46	43.11
30 July 2014	0.87	36.44	15.29
06 Augt 2014	0.89	60.09	27.02
13 Augt 2014	0.74	37.03	-2.88
20 Augt 2014	0.81	49.74	18.37
27 Augt 2014	0.81	47.38	24.96
03 Sept 2014	0.72	58.64	19.92
10 sep 2014	0.90	25.70	-1.44
All 10 weeks	0.78	46.64	21.26

The Table 3 shows a highest correlation between H-E rain WWR rain of 0.90 for a week from 4 to 10 September 2014 and lowest correlation of 0.64 for a week from 10 to 16 July 2014. In order to see the comparison results in better perspectives, we have also used TRMM 3B42 V7 observations and compared their weekly met-subdivision averaged values with corresponding H-E and WWR rain values. This is shown in Table 4 below.

Table 4: Week-by-Week comparison statistics of weekly meteorological subdivision averaged 3B42 V7 rain with IMD WWR and H-E rain.

Week ending on	3B42 vs WWR			3B42 Vs HE		
	R	Err	Bias	R	Err	Bias
9 July 2014	0.53	57.24	0.32	0.49	70.94	-19.59
16 July 2014	0.91	58.67	-18.63	0.91	81.48	-45.65
23 July 2014	0.82	23.98	1.94	0.86	40.23	-18.35
30 July 2014	0.61	45.63	-4.66	0.48	44.90	-3.22
06 Augt 2014	0.52	50.53	-17.23	0.63	38.00	-14.34
13 Augt 2014	0.92	49.09	1.66	0.86	68.90	-46.32
20 Augt 2014	0.82	30.17	-7.46	0.87	53.34	-25.83
27 Augt 2014	0.82	43.01	-5.20	0.61	97.40	-48.31
03 Sept 2014	0.77	51.67	22.68	0.92	29.32	-2.28
10 sep 2014	0.93	24.83	-8.11	0.88	39.21	-23.40
All 10 weeks	0.78	45.15	-3.47	0.76	60.19	-24.73

If we compare Table 3 and 4, we may conclude that overall (with all 10 weeks of dataset) correlation of WWR with H-E is same as that with TRMM 3B42 V7. The rms difference of WWR with H-E is also very close to that with TRMM 3B42 V7. Despite of these similarities, there is remarkable difference between these 2 comparisons, that is, the correlation between H-E and WWR varies from moderate a range of 0.64 to 0.90, whereas that between TRMM 3B42 V7 and WWR varies from low value of 0.52 to high value of 0.93. Thus statistics between H-E and WWR is more stable compared to that between TRMM 3B42 V7 and WWR. The comparison between TRMM 3B42 V7 and H-E is also attempted and is shown in the Table 4.

It may be recalled that 3B42 V7 is from state-of-art algorithm that combines IR and Microwave Measurements and adjust the biases with surface observations. Despite of these facts, H-E results are comparable (or even better) to that of 3B42 V7 measurements. In order to see that how modified H-E measurements compare with only Microwave measurements of precipitation, we compared 2 weeks (3 – 16 July 2014) of weekly met-subdivisions averaged H-E rain with TRMM 3B41RT. The comparison results are shown in Table 5 below. The comparison shows poorer correlation between 3B41 and WWR that that between H-E and WWR. Thus, modified H-E rain is having a better representation of the surface observations than that by only microwave based rain rates from TRMM 3B41RT.

Table 5: Week-by-Week comparison statistics of weekly meteorological subdivision averaged rain from 3B41RT with H-E rain with WWR and IMD.

Week ending on	3B41 vs WWR			3B41 Vs HE		
	R	Err	Bias	R	Err	Bias
9 July 2014	0.66	47.46	24.88	0.81	34.75	4.58
16 July 2014	0.56	88.98	23.69	0.78	65.72	-24.29
All 2 weeks	0.58	71.31	24.28	0.80	52.56	-9.86

We are also obtained 0.25°x0.25° daily gridded surface rain measurements from IMD. Before using them for further comparisons in finer spatial and temporal scales, we examined their integrity vis-à-vis rain values provided in WWR. We averaged gridded rain values and generated weekly rain maps similar to those provided in WWR. The comparison statistics of IMD gridded dataset with WWR is provided in Table 6 below:

Table 6: Comparison statistics of weekly meteorological subdivision averaged 0.25°x0.25° daily gridded surface rain measurements from IMD with WWR.

	IMD daily gridded data versus IMD Weekly Weather Report		
All 10 Weeks	R = 0.97	rmse = 16.36	Bias = -0.37

We expect a near perfect comparison between IMD gridded data and IMD WWR but there exists marked difference between them.

The Table 3 shows the comparison between rain values from modified H-E and WWR, but that does not give any indication of performance of H-E in different meteorological sub-divisions. In Table 7, we have made comparison in different subdivisions and presented the statistics. Herein comparison over Lakshadweep is not provided as that is considered to represent maritime environment. It can be observed that high correlation exist in all the subdivisions except in Nagaland, Manipur, Meghalaya and Tripura (NMMT) and Coastal AP, which needs further investigation. Similar comparison between 3B42 V7 and modified H-E is also attempted, which is shown in Table 8. From Table 8, it can be observed that the correlation of modified H-E rain with 3B42 V7 over NMMT and Coastal Andhra Pradesh (AP) is 0.32 and 0.64 which is not as poor as in Table 7. Thus any study to understand large difference in these two met subdivisions in Table 7 needs to take cognition of this fact that the 3B42 V7 and H-E are uniformly measured spatially averaged measurements. The coarser correlation as observed in Table 7 in NMMT and Coastal AP may be due to high variability of precipitation in these regions associated with geolocation error in the INSAT-3D observations (mean error of 1-2 pixel error is possible) which may show poorer comparison with surface observations taken at fixed locations (Piyush et al., 2012). Other than these two regions the correlation between rain from modified H-E and WWR is reasonably good, especially in the regions with high altitudes like J & K, Arunachal Pradesh, Uttarakhand and Himachal Pradesh, etc.

Table 7: Comparison statistics of weekly averaged rain from H-E and WWR in each met subdivisions.

Met Sub Division	R	rmse	bias	Met Sub Division	R	rmse	bias
A & N	0.48	75.60	-55.50	West MP	0.63	74.80	-33.61
Arunachal Pradesh	0.73	63.23	-32.03	East MP	0.71	94.62	-58.28
Assam & Megha.	0.69	49.90	-37.88	Guj, DNH & Dam.	0.76	40.61	10.15
NMMT	-0.07	61.06	-37.03	Saur., Katch & Diu	0.89	13.92	1.21
SHWB	0.35	53.47	-0.99	Konkan & Goa	0.62	138.24	92.14
Gangetic WB	0.57	73.65	-17.54	Madhya Maha	0.81	69.72	-48.06
Orissa	0.94	37.25	-30.85	Marathwada	0.71	64.50	-44.66
Jharkhand	0.75	67.34	-52.02	Vidarbh	0.86	44.42	-26.58
Bihar	0.94	29.23	-19.52	Chattisgarh	0.91	48.28	-33.79
East UP	0.89	39.61	-28.65	Coastal AP	0.22	41.64	-33.33
West UP	0.87	28.32	-20.28	Telengana	0.72	33.99	-23.12
Uttarakhand	0.84	43.35	-19.98	Rayalaseema	0.89	13.44	-10.87
HR., Chd. & Delhi	0.61	16.55	-8.77	TN & Pondicherry	0.73	20.36	-16.96
Punjab	0.97	10.42	-4.65	Coastal Karnataka	0.82	129.69	-60.61
HP	0.72	34.71	-21.01	N.I. Karnataka	0.94	31.03	-22.05
J & K	0.98	15.15	3.60	S.I. Karanataka	0.73	41.82	-33.94
West Raj	0.85	21.92	-12.86	Kerala	0.79	62.98	14.51
East Raj	0.77	40.61	-20.38				

In order to present the results in proper prospective, the tables similar to Table 7 and 8 providing comparison statistics between TRMM 3B42 V7 and WWR is provided in Table 9 below. Again one can see poorer comparison of TRMM 3B42 V7 with WWR rain over NMMT and Coastal Andhra Pradesh.

Table 8: Comparison statistics of weekly averaged rain from H-E and 3B42 V7 in each met subdivisions.

Met Sub Division	R	rmse	bias	Met Sub Division	R	rmse	bias
A & N	0.37	101.71	85.38	West MP	0.92	51.96	30.53
Arunachal Pradesh	0.68	84.80	59.63	East MP	0.87	88.81	55.74
Assam & Megha.	0.35	47.45	20.53	Guj, DNH & Dam.	0.96	37.48	-21.96
NMMT	0.32	45.98	21.92	Saur., Katch & Diu	0.91	27.57	-12.09
SHWB	0.30	47.84	14.24	Konkan & Goa	0.79	76.09	-23.42
Gangetic WB	0.89	58.24	24.54	Madhya Maha	0.86	55.00	37.13
Orissa	0.92	45.07	38.07	Marathwada	0.86	35.85	17.08
Jharkhand	0.77	72.68	59.75	Vidarbh	0.88	36.12	15.48
Bihar	0.86	38.42	18.10	Chattisgarh	0.92	59.78	40.81
East UP	0.60	39.14	11.87	Coastal AP	0.64	27.84	20.81
West UP	0.87	19.07	1.01	Telengana	0.66	29.18	10.79
Uttrakhand	0.93	47.52	28.65	Royalaseema	0.89	11.96	4.73
HR., Chd. & Delhi	0.52	20.66	-2.78	TN & Pondicherry	0.83	12.87	8.63
Punjab	0.72	36.76	-17.67	Coastal Karnataka	0.64	205.93	140.00
HP	0.85	36.99	25.87	N.I. Karnataka	0.81	29.56	16.78
J & K	0.95	50.41	25.75	S.I. Karanataka	0.45	56.81	46.01
West Raj	0.70	24.40	10.28	Kerala	0.81	51.80	37.02
East Raj	0.86	33.51	16.33				

Table 9: Comparison statistics of weekly averaged rain from 3B42 V7 and WWR in each met subdivisions.

Met Sub Division	R	rmse	bias	Met Sub Division	R	rmse	bias
A & N	0.56	49.75	29.88	West MP	0.73	35.85	-3.08
Arunachal Pradesh	0.93	42.19	27.60	East MP	0.84	28.70	-2.54
Assam & Megha.	0.60	34.61	-17.35	Guj, DNH & Dam.	0.75	48.01	-11.81
NMMT	0.34	28.77	-15.10	Saur., Katch & Diu	0.80	30.94	-10.89
SHWB	0.82	32.98	13.25	Konkan & Goa	0.53	130.65	68.72
Gangetic WB	0.58	28.29	7.00	Madhya Maha	0.61	36.98	-10.92
Orissa	0.95	24.12	7.23	Marathwada	0.60	48.07	-27.58
Jharkhand	0.85	18.36	7.74	Vidarbh	0.98	17.21	-11.10
Bihar	0.83	27.10	-1.42	Chattisgarh	0.91	28.15	7.02
East UP	0.66	28.19	-16.78	Coastal AP	0.54	18.64	-12.52
West UP	0.92	21.84	-19.26	Telengana	0.74	23.69	-12.33

Uttrakhand	0.95	22.32	8.66	Royalaseema	0.92	12.70	-6.14
HR., Chd. & Delhi	0.78	18.92	-11.55	TN & Pondicherry	0.96	10.28	-8.33
Punjab	0.74	40.08	-22.32	Coastal Karnataka	0.69	123.65	79.39
HP	0.76	15.45	4.86	N.I. Karnataka	0.82	22.51	-5.27
J & K	0.97	57.95	29.35	S.I. Karanataka	0.47	29.01	12.07
West Raj	0.78	12.92	-2.58	Kerala	0.67	87.37	51.53
East Raj	0.61	37.03	-4.05				

The above comparisons are carried out in weekly meteorological sub-division scales. The rain is known to have variability from few meters to continental scales and from few seconds to any time scale. In shorter measuring scales, it behaves as quasi-random stochastic process. Therefore, rain comparisons in shorter time scales and from observations in different spatial scales lead to large errors (Piyush et al., 2012). Nevertheless, we have compared daily $0.25^{\circ} \times 0.25^{\circ}$ averaged rain from modified H-E method with gridded dataset from IMD. The comparisons are carried out for each of the met subdivisions as provided in Table 7 to table 9. The comparison statistics is provided in Table 10.

The Table 10 shows a reasonable good comparison statistics for different regions. If all regions are considered together, the comparison shows a correlation of 0.47 and rmse of 25.40 mm/day. In order to see this statistics in proper prospective, similar comparison statistics of rain from TRMM 3B42 V7 and IMD gridded dataset is provided in Table 11, which show slightly improved correlation of 0.53 and rmse of 19.30 mm/day. The difference may be due to geolocation error is INSAT-3D which is suspected to have mean error of 1-2 pixels in geolocation due to anomaly in the star sensor, which has potential to degrade statistics in smaller scales.

Table 10: Comparison statistics of $0.25^{\circ} \times 0.25^{\circ}$ daily gridded rain from H-E and IMD in each met subdivisions.

Met Sub Division	R	rmse	bias	Met Sub Division	R	rmse	bias
Arunachal Pradesh	0.26	43.63	-5.87	East MP	0.45	30.11	-7.24
Assam & Megha.	0.52	46.41	-3.34	Guj, DNH & Dam.	0.42	19.02	1.66
NMMT	0.17	28.77	-6.89	Saur., Katch & Diu	0.39	13.54	0.43
SHWB	0.22	38.85	0.84	Konkan & Goa	0.44	43.31	8.26
Gangetic WB	0.41	23.45	-4.51	Madhya Maha	0.39	34.42	-7.83
Orissa	0.51	31.85	-5.05	Marathwada	0.46	27.38	-6.36
Jharkhand	0.57	26.48	-8.14	Vidarbh	0.57	23.43	-3.93
Bihar	0.63	18.70	-2.30	Chattisgarh	0.61	26.18	-5.55
East UP	0.56	20.82	-4.61	Coastal AP	0.32	25.28	-4.64
West UP	0.45	16.03	-2.86	Telengana	0.40	18.04	-2.77
Uttrakhand	0.36	34.28	-3.33	Royalaseema	0.51	9.15	-1.17
HR., Chd. & Delhi	0.39	10.43	-1.25	TN & Pondicherry	0.34	12.65	-2.46

Punjab	0.45	9.16	0.21	Coastal Karnataka	0.51	47.31	-3.04
HP	0.30	31.83	-2.97	N.I. Karnataka	0.42	16.94	-2.38
J & K	0.34	15.06	-1.28	S.I. Karanataka	0.54	21.76	-5.62
West Raj	0.54	11.78	-1.98	Kerala	0.47	28.09	-1.00
East Raj	0.54	19.79	-2.93	All regions	0.47	25.40	-3.24
West MP	0.42	25.20	-3.71				

Table 11: Comparison statistics of 0.25°x0.25° daily gridded rain from TRMM-3B42 V7 and IMD in each met subdivisions.

:

Met Sub Division	R	rmse	bias	Met Sub Division	R	rmse	bias
Arunachal Pradesh	0.42	24.04	3.37	East MP	0.60	14.67	0.33
Assam & Megha.	0.56	28.02	0.31	Guj, DNH & Dam.	0.61	20.14	-0.77
NMMT	0.26	15.75	-2.33	Saur., Katch & Diu	0.57	16.03	-1.09
SHWB	0.39	24.06	3.57	Konkan & Goa	0.55	38.99	9.71
Gangetic WB	0.43	14.67	-0.41	Madhya Maha	0.51	21.11	-2.51
Orissa	0.62	22.52	-0.15	Marathwada	0.58	14.10	-3.22
Jharkhand	0.51	15.63	-0.13	Vidarbh	0.74	14.98	-1.45
Bihar	0.60	15.53	0.54	Chattisgarh	0.62	18.73	0.96
East UP	0.51	17.44	-2.31	Coastal AP	0.50	11.79	-1.14
West UP	0.57	12.07	-1.90	Telengana	0.55	11.42	-0.51
Uttrakhand	0.57	16.72	1.67	Royalaseema	0.62	7.50	-0.87
HR., Chd. & Delhi	0.53	7.88	-0.75	TN & Pondicherry	0.53	8.97	-1.33
Punjab	0.38	10.26	-0.45	Coastal Karnataka	0.60	36.46	10.83
HP	0.50	12.93	1.47	N.I. Karnataka	0.51	13.19	-0.91
J & K	0.43	6.06	0.04	S.I. Karanataka	0.58	14.61	-0.35
West Raj	0.58	7.67	-0.05	Kerala	0.55	23.91	4.18
East Raj	0.64	14.66	-0.16	All regions	0.53	19.30	1.65
West MP	0.60	16.34	-0.07				

A comparison of rain from modified H-E and TRMM-3B42 V7 in 0.25°x0.25° degree in each met subdivision is shown in Table 12, which show significantly higher correlations and smaller rmse for most of the regions. This is mainly due to spatially averaged measurement of rain from H-E and TRMM TRMM-3B42 V7. The Table 12 also shows the performance of modified H-E with respect to TRMM 3B42 V7 over oceans. It may be noted here that neither IMD WWR nor gridded dataset has provides measurements over oceans. So the comparison with TRMM 3B42 V7 is the only source for accessing the quality of H-E rain over oceans. It may be noted from Table 12 that daily 0.25°x0.25° gridded rain from H-E and 3B42 RT has a good agreement over oceans with correlation of 0.65 and rmse of 15.88 mm/day. If all area including land and oceans including and surrounding India are taken into consideration, the correlation and rmse between H-E and TRMM-3B42 V7 is 0.59 and rmsd of 22.44 mm/day.

Table 12: Comparison statistics of 0.25°x0.25° daily gridded rain from H-E and TRMM 3B42 V7 in each met subdivisions.

Met Sub Division	R	rmse	bias	Met Sub Division	R	rmse	bias
Arunachal Pradesh	0.51	37.82	9.11	Guj, DNH & Dam.	0.58	20.43	-2.42
Assam & Megha.	0.61	40.53	3.55	Saur., Katch & Diu	0.66	14.67	-2.04
NMMT	0.39	25.09	4.31	Konkan & Goa	0.67	34.83	0.68
SHWB	0.37	34.26	2.61	Madhya Maha	0.71	26.84	5.59
Gangetic WB	0.57	20.69	3.89	Marathwada	0.71	21.00	3.29
Orissa	0.57	30.05	4.69	Vidarbh	0.73	19.33	3.05
Jharkhand	0.62	25.59	7.93	Chattisgarh	0.66	24.44	6.25
Bihar	0.68	16.77	2.75	Coastal AP	0.53	22.76	3.33
East UP	0.73	16.74	2.22	Telengana	0.55	15.78	2.24
West UP	0.59	14.08	0.91	Rayalaseema	0.60	8.27	0.32
Uttrakhand	0.50	31.89	4.83	TN & Pondicherry	0.48	11.47	1.15
HR., Chd. & Delhi	0.45	10.53	0.17	Coastal Karnataka	0.49	49.59	13.70
Punjab	0.47	8.46	-0.63	N.I. Karnataka	0.51	16.72	1.75
HP	0.50	26.72	4.22	S.I. Karanataka	0.46	24.12	5.35
J & K	0.34	14.14	1.28	Kerala	0.51	27.64	4.40
West Raj	0.65	10.51	1.97	Oceans	0.65	15.88	-1.09
East Raj	0.67	16.71	2.87	Land outside India	0.33	46.52	10.53
West MP	0.60	21.62	4.18	All regions	0.59	22.44	3.28
East MP	0.62	28.30	8.01				

7.0 Conclusions and Expected Accuracy

The results provided above indicate reasonably good agreement of INSAT-3D H-E rain with surface observations. The changes that are carried out in the modified algorithm are able to successfully represent the orographic rain which otherwise was not found to suffer from huge errors. The rain is highly variable parameter over space and time and its validation in smaller scales always resulting large huge errors (Piyush et al., 2012). The results presented above should be viewed with respect to validation comparison results of the global standard rain products by other researchers. For example, in a recent study by Tan et al. (2015) in which they evaluated six high resolution precipitation products including TRMM-3B42 V7 over the Malaysia. They reported that among 5 satellite based rain products, the 3B42 V7 and is the best performing with respect to surface observations, which on daily scale provides a correlation of 0.39 and rmse of 18.35 mm/day. While the India has much more diverse surface and climatic conditions with different cloud types and wide range of precipitation rates during S-W months, we achieve much higher correlation between modified H-E rain with surface observations. A more important aspect of the rain from H-E vis-à-vis TRMM 3B42 V7 is timely availability of H-E product from IMD and MOSDAC sites. The TRMM 3B42 V7 is available after latency of about 4 months, whereas INSAT-3D H-E is available within 15

minutes of data acquisition, which makes H-E very important for operational users, especially those working with rain related natural disasters, nowcasting and numerical weather predictions.

Based on above analysis, we can summarize the results as follows:

1. H-E in the present form performs well over most parts of land and oceans but has found to have weakness over high altitude regions.
2. The weakness of the H-E in high altitude areas is successfully addressed in modified H-E.
3. On weekly and met-subdivision scale, the modified H-E provides a correlation of 0.78 and rms difference of 46.64 mm with surface observations from IMD weekly Weather Report (WWR).
4. On weekly and met-subdivision scale, the modified H-E provides a correlation of 0.78 and rms difference of 45.15 mm with TRMM 3B42 V7.
5. It is found that comparison statistics between modified H-E and WWR is comparable to that between TRMM-3B42 V7 and WWR. However, week-by-week variation in the comparison statistics of H-E versus WWR is more stable than that between TRMM 3B42 V7 and WWR.
6. Daily $0.25^{\circ} \times 0.25^{\circ}$ gridded rain from modified H-E matches well with surface gridded observations over land with correlation of 0.47 and rms difference of 25.40 mm/day. Slightly higher correlation of 0.59 and rms of 22.40 difference mm/day is observed when H-E rain is compared with TRMM 3B42 V7. The results are in tune with comparison between 3B42 V7 with surface observations.
7. The comparison over oceans is not possible with IMD gridded surface observations hence comparison is done with daily $0.25^{\circ} \times 0.25^{\circ}$ gridded rain for modified H-E and TRMM 3B42 V7 and that show a correlation of 0.65 and rms difference of 15.88 mm/h.
8. The H-E rain shows a good comparison in all the met subdivisions except in “Nagaland, Manipur, Meghalaya and Tripura (NMMT)” and “Coastal Andhra Pradesh”, which are also poorly comparable with TRMM 3B42 V7. The reason needs to be further investigated.
9. Over all, rain from modified H-E is comparable to TRMM 3B42 V7 with an advantage of near real time availability of measurements (within 30 minutes) compared to 4 months for the availability of TRMM 3B42 V7 product.

The modified H-E is soon going to be made operational both at SAC and MOSDAC sites. A “Algorithm Theoretical Basis Document” is presently under preparation.

8.0 Implementation Steps

The modified H-E is already implemented offline and running flawlessly. The present operational structure of H-E module comprising of two main programs called HEM and HEG. The HEM takes Earth elevation model (ETOPO2) as static data input and NCEP GFS model file as dynamic input and provides the correction files for equilibrium level,

orography, TPW and RH. The HEM uses three separate programs as subroutines for orographic correction, wind interpolation and an atmospheric thermodynamic model for the calculation of LNB/EL. The HEG takes INSAT-3D level1 files as input along with correction files to produce the rain at every pixel within the study area. This is illustrated in flow chart 1 (Fig. 17). In the modified scheme, new HEM removes the program for atmospheric thermodynamics and includes the necessary model equations in the main body of HEM itself. The modified HEM also takes histogram equalization matched up files for each of the height bins of the parameter (TPW/RH) at surface to given elevation bin as static input files. The only change in input to HEG is that in modified program for H-E rain, it also takes as input to Earth elevation model file (ETOPO2). This is shown in Fig. 18.

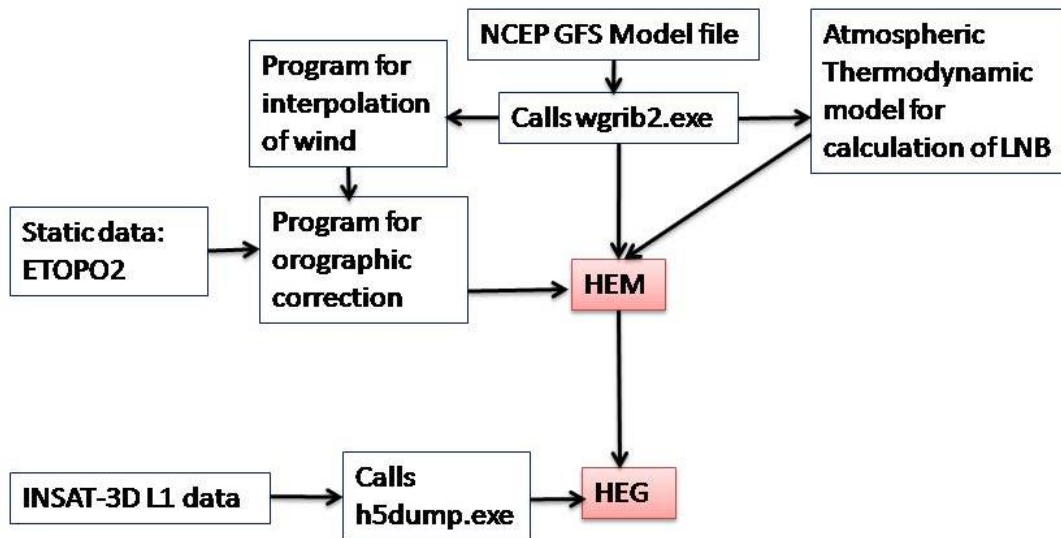


Fig. 17: Flow chart showing present structure of H-E module.

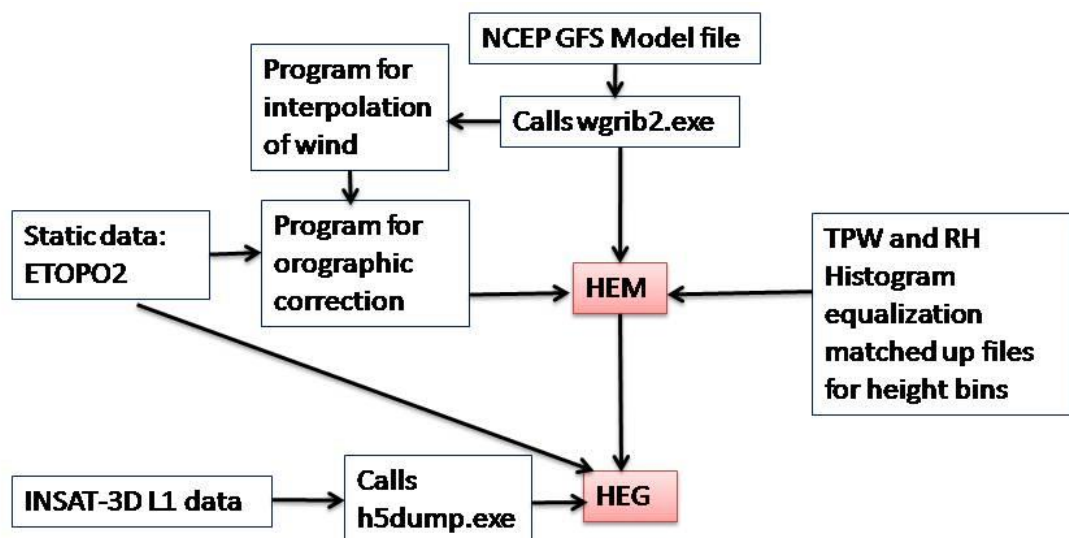


Fig. 18: Flow chart showing modified structure of H-E module.

9.0 Domain and the format of output

The output is provided in terms of geolocation (latitude and longitude) and rain rate in mm/h.

The area of coverage is latitude: 30°E to 130° E, and longitude: 50° S to 50° N.

10.0 Acknowledgement

Authors are thankful to Dr. Robert Koligowski, NOAA/STAR for his unconditional support to develop H-E at SAC.

11.0 References

- Anonymous, 2014, Tropical Cyclone Phailin – Prediction, Monitoring and Analysis of Aftereffects, Report # SAC/EPSA/SR-01/2014, Pub. by EPSA/SAC, ISRO, ahmedabad, p 200.
- Arkin, P A, A V R Krishna Rao, RR Kelker, 1986, Large scale precipitation and outgoing longwave radiation from INSAT-1B during 1986 South-West Monsoon, Season, *Journal of Climate*, 2, 619-628.
- Barrett, E. c., and D. W. Martin, 1981, The use of satellite data in rainfall monitoring. Academic Press, New York, 340 pp.
- Bhandari, S.M and A.K. Varma, 1995, On Estimation of Large Scale Monthly Rainfall Estimation Over the Indian Region Using Minimal INSAT-VHRR Data, *International Journal of Remote Sensing*, 16, 2023-2030.
- Piyush, D N, A K Varma, P K Pal and G Liu, 2012, An Analysis of Rainfall Measurements over Different Spatio-Temporal Scales and Potential Implications for Uncertainty in Satellite Data Validation, *Journal of Meteorological Society of Japan*, 90 (4), DOI: 10.2151/JMSJ.2012-408.
- Scofield, R. A., 1987. The NESDIS operational convective precipitation estimation technique. *Mon. Wea. Rev.*, 115, 1773–1792.
- Scofield, R. A., and Kuligowski, 2003, Status and outlook of operational satellite precipitation algorithms for extreme-precipitation events, *Weather and Forecasting*, 18, 1037-1051.
- Varma, A. K. and G. Liu, 2010, On Classifying Rain Types Using Satellite Microwave Observations, *Journal of Geophysical Research*, 115, D07204, doi:10.1029/2009JD012058.
- Varma, A. K., and G. Liu, 2006, Small-Scale Horizontal Rainrate Variability by Satellite, *Monthly Weather Review*, 134 (10), 2722-2733.
- Varma, A K and P K Pal, 2012, Use of TRMM Precipitation Radar to address the problem of rain detection in Passive Microwave Measurements, *Indian Journal of Radio and Space Physics*, 41 411-420.
- Varma, A. K., G. Liu, and Y. J., Noh, 2004, Sub-Pixel Scale Variability of Rainfall and Its Application to Mitigate the Beam-Filling Problem, *Journal of Geophysical Research*, 109, D18210, doi:10.1029/2004JD004968.
- Varma, A. K., and R.M. Gairola, 2007, Algorithm Theoretical Basis Document for Hydro-estimator Method, in “INSAT Geophysical Parameter Retrieval System – ATBD Document”, report# SAC/IMDPS/TN-05/Version-1, pp 62-78.
- Vicente, G. A., J. C. Davenport, and R. A. Scofield, 2002, The role of orographic and parallax corrections on real time high resolution satellite rainfall estimation. *Int. J. Remote Sens.*, 23, 221-230.
- Vicente, G A, R A Scofield, and W P Menzel, 1998, The Operational GOES Infrared Rainfall Estimation Technique, *Bul. of American Met. Soc.*, 79 (9), 1883.